PDE Project Report

Mean field game with congestion effect

M2MO

2024-2025

Authors: *Id :*

BERARD Stanislas 22411006

THOMASSIN Pablo 22423686

Course Coordinator:

Yves ACHDOU and Olivier BOKANOWSKY

4th March 2025

Contents

1 Abstract

This report presents a comprehensive study of Mean Field Games (MFGs) with a focus on the interplay between the Hamilton-Jacobi-Bellman (HJB) equation and the Kolmogorov-Fokker-Planck (KFP) equation. We formulate the MFG problem on a finite time horizon with a state space in dimension d , incorporating running and terminal cost functions. The problem is characterized by a forward-backward system of partial differential equations (PDEs), where the HJB equation governs the optimal control of individual agents, and the KFP equation describes the evolution of the population density. We propose a discrete approximation scheme using finite differences and develop a fixed-point algorithm to solve the coupled system iteratively. Key theoretical results include the uniqueness of solutions for the discrete HJB and KFP equations, as well as the propagation of positivity in the population density. Numerical experiments are conducted to validate the proposed methodology, and the results are analyzed under various parameter settings. The study concludes with a discussion on the implications of the Hamiltonian structure and its impact on the convergence and stability of the numerical scheme.

2 Introduction

Mean Field Games (MFGs) have emerged as a powerful framework for analyzing the behavior of large populations of interacting agents in strategic environments. Introduced by Lasry and Lions, MFGs provide a mathematical foundation for understanding how individual decision-making influences, and is influenced by, the collective behavior of the population. The MFG framework is particularly useful in economics, finance, and engineering, where it has been applied to model phenomena such as crowd dynamics, market equilibria, and resource allocation.

At the heart of MFGs lies a coupled system of PDEs: the Hamilton-Jacobi-Bellman (HJB) equation, which describes the optimal control strategy for an individual agent, and the Kolmogorov-Fokker-Planck (KFP) equation, which governs the evolution of the population density. The HJB equation is backward in time, reflecting the agent's optimization problem, while the KFP equation is forward in time, capturing the macroscopic behavior of the population. The coupling between these equations arises from the fact that the optimal control depends on the population density, and the population density evolves according to the agents' strategies

3 Methodology and Results

3.1 Methodology

3.1.1 Mean Field Game Exposition

We fix a finite time horizon $T > 0$. We will work on the state space $\mathbb{R}^d$. Let

$$f : \mathbb{R}^d \times \mathbb{R} \times \mathbb{R}^d \to \mathbb{R}, \quad (x, m, \gamma) \mapsto f(x, m, \gamma),$$
$$\varphi : \mathbb{R} \times \mathbb{R} \to \mathbb{R}, \quad (x, m) \mapsto \varphi(x, m)$$

be respectively a running cost and a terminal cost, on which assumptions will be made later on.

We consider the following Mean Field Game: find a flow of probability densities $\hat{m}$: $[0, T] \times \mathbb{R}^d$ (denoted $\hat{m} \in M$) and a feedback control $\hat{v} : [0, T] \times \mathbb{R}^d \to \mathbb{R}^d$ (denoted $\hat{v} \in V$) satisfying the following two conditions:

- $\hat{v}$ minimizes

$$J_{\hat{m}}(v) = \mathbb{E}\left[\int_0^T f\left(X_t^v, \hat{m}(t, X_t^v), v(t, X_t^v)\right) dt + \varphi\left(X_T^v, \hat{m}(T, X_T^v)\right)\right], \tag{1}$$

  subject to the constraint that $X^v = (X_t^v)_{t\geq 0}$ solves the stochastic differential equation (SDE):

$$dX_t^v = b\left(X_t^v, \hat{m}(t, X_t^v), v(t, X_t^v)\right) dt + \sigma dW_t, \quad t \geq 0, \tag{2}$$

  where $\sigma > 0$ is the volatility, $b : \mathbb{R}^d \times \mathbb{R} \times \mathbb{R}^d \to \mathbb{R}^d$ is a given function, and X_0^v is an independent random variable in $\mathbb{R}^d$, distributed according to law m_0.

- For all $t \in [0, T]$, $\hat{m}(t, \cdot)$ is the law of X_t^v.

3.1.2 Kolmogorov-Fokker-Planck Equation

It is useful to note that for a given feedback control v, the density m_t^v of the law of X_t^v following equation (3) solves the Kolmogorov-Fokker-Planck (KFP) equation:

$$\partial_t m^v(t,x) - \nu \Delta m^v(t,x) + \nabla \cdot (m^v(t,\cdot) b(\cdot, m^v(t,\cdot), v(t,\cdot)))(x) = 0, \quad (t,x) \in (0,T] \times \mathbb{R}^d, \tag{3}$$

with initial condition

$$m^v(0,x) = m_0(x), \quad x \in \mathbb{R}^d, \tag{4}$$

where $\nu = \sigma^2/2$.

3.1.3 Differential Operators

We recall the definition of the Laplacian Δ and Divergence $\nabla\cdot$ operators for smooth functions $\psi : \mathbb{R}^d \to \mathbb{R}$ and $V : \mathbb{R}^d \to \mathbb{R}^d$:

$$\Delta \psi(x) = \sum_{i=1}^d \partial_{x_i}^2 \psi(x), \tag{5}$$

$$\nabla \cdot V(x) = \sum_{i=1}^d \partial_{x_i} V_i(x), \tag{6}$$

where V_i denotes the i-th coordinate of V. Additionally, we define the Gradient ∇ and the Hessian ∇^2:

$$\nabla \psi(x) = (\partial_{x_1} \psi(x), \ldots, \partial_{x_d} \psi(x))^T, \tag{7}$$

$$\nabla^2 \psi(x) = (\partial_{x_i x_j}^2 \psi(x))_{1 \le i,j \le d}. \tag{8}$$

3.1.4 Hamilton-Jacobi-Bellman Equation

The control problem faced by an infinitesimal player can be addressed using standard optimal control theory. Let u be the value function of the above optimal control problem for a typical player, namely:

$$u(t,x) = \inf_{v \in V} J_{\hat{m}}(t,x,v), \tag{9}$$

where

$$J_{\hat{m}}(t,x,v) = \mathbb{E}\left[\int_t^T f(X_s^{t,x,v}, \hat{m}(s, X_s^{t,x,v}), v(s, X_s^{t,x,v}))ds + \varphi(X_T^{t,x,v}, \hat{m}(T, X_T^{t,x,v}))\right]. \tag{10}$$

The value function u satisfies the Hamilton-Jacobi-Bellman (HJB) equation:

$$\partial_t u(t,x) + \nu\Delta u(t,x) - H(x, m(t,x), \nabla u(t,x)) = 0, \quad (t,x) \in [0,T) \times \mathbb{R}^d, \tag{11}$$

with terminal condition

$$u(T,x) = \varphi(x, m(T,x)), \quad x \in \mathbb{R}^d, \tag{12}$$

where the Hamiltonian H is defined as:

$$H(x,m,p) = \sup_{\gamma \in \mathbb{R}^d} \left[-f(x,m,\gamma) - \langle b(x,m,\gamma), p\rangle\right]. \tag{13}$$

Finally, (u,m) solves the following forward-backward PDE system:

$$-\partial_t u - \nu\Delta u + H(x,m,\nabla u) = 0, \quad (t,x) \in [0,T) \times \mathbb{R}^d, \tag{14}$$

$$\partial_t m - \nu\Delta m - \nabla \cdot (m\nabla_p H(\cdot, m, \nabla u)) = 0, \quad (t,x) \in (0,T] \times \mathbb{R}^d. \tag{15}$$

3.1.5 Hamiltonian assumptions

Since $H_0(p,\mu) = \frac{1}{\beta}\frac{|p|^\beta}{(c_0+c_1\mu)^\alpha}$, a sensible choice for the discrete Hamiltonian is

$$\tilde{H}(p_1,p_2,\mu) = \frac{1}{\beta}\frac{\left((p_1)_-^2 + (p_2)_+^2\right)^{\frac{\beta}{2}}}{(c_0+c_1\mu)^\alpha}, \tag{16}$$

where X_+, resp. X_- stand for the positive (resp. negative) part of X: $X = X_+ - X_-$ and $|X| = X_+ + X_-$, and where we set $X_+^2 = (X_+)^2$ and $X_-^2 = (X_-)^2$.

The monotonicity of the discrete Hamiltonian guarantees uniqueness in the discrete HJB equations and discrete KFP equations below. It also guarantees that the solution of the discrete

KFP equation below is non-negative if its initial condition is non-negative.

The consistency of the discrete Hamiltonian is a key ingredient for convergence of the discrete schemes. The differentiability of the discrete Hamiltonian makes it possible to use Newton's method for solving the discrete HJB equation.

3.1.6 Finite differences

Let N_T and N_h be two positive integers. We consider $N_T + 1$ and N_h points in time and space respectively. Set $\Delta t = \frac{T}{N_T}$, $h = \frac{1}{N_h - 1}$, and $t_n = n \cdot \Delta t$, $x_i = i \cdot h$ for $(n, i) \in \{0, \dots, N_T\} \times \{0, \dots, N_h - 1\}$. We approximate u and m respectively by vectors U and M in $\mathbb{R}^{(N_T+1)\times N_h}$, that is,

$$u(t_n, x_i) \approx U_i^n \quad \text{and} \quad m(t_n, x_i) \approx M_i^n \tag{17}$$

for each (n, i) in $\{0, \dots, N_T\} \times \{0, \dots, N_h - 1\}$.

To take into account Neumann boundary conditions, we introduce ghost nodes $x_{-1} = -h$, $x_{N_h} = 1 + h$ and set:

$$U_{-1}^n = U_0^n, \quad U_{N_h}^n = U_{N_h-1}^n, \quad M_{-1}^n = M_0^n, \quad M_{N_h}^n = M_{N_h-1}^n. \tag{18}$$

We introduce the following finite difference operators:

$$\partial_t w(t_n, x) \leftrightarrow (D_t W)^n = \frac{W^{n+1} - W^n}{\Delta t}, \quad n \in \{0, \dots, N_T - 1\}, W \in \mathbb{R}^{N_T+1}, \tag{19}$$

$$\partial_x w(t, x) \leftrightarrow (DW)_i = \frac{W_{i+1} - W_i}{h}, \quad i \in \{0, \dots, N_h - 1\}, W \in \mathbb{R}^{N_h}, \tag{20}$$

$$\partial_{xx} w(t, x_i) \leftrightarrow (\Delta_h W)_i = \frac{W_{i+1} - 2W_i + W_{i-1}}{h^2}, \quad i \in \{0, \dots, N_h - 1\}, W \in \mathbb{R}^{N_h}. \tag{21}$$

Defining gradient operators:

$$[\nabla_h W]_i = ((DW)_i, (DW)_{i-1}), \quad i \in \{0, \dots, N_h - 1\}, W \in \mathbb{R}^{N_h}. \tag{22}$$

Considering a matrix $W \in \mathbb{R}^{(N_T+1)\times N_h}$, we define:

$$\partial_x W \leftrightarrow \frac{1}{h}\begin{bmatrix} -1 & 1 & 0 & \cdots & 0 \\ 0 & -1 & 1 & \cdots & 0 \\ \vdots & \vdots & \vdots & \ddots & \vdots \\ 0 & 0 & \cdots & -1 & 1 \\ 0 & 0 & \cdots & 0 & 0 \end{bmatrix} W. \tag{23}$$

This matrix will further be denoted as D (as written in the Python code)

Taking into account Neumann conditions:

$$\partial_{xx} W \leftrightarrow \frac{1}{h^2}\begin{bmatrix} -1 & 1 & 0 & \cdots & 0 \\ 1 & -2 & 1 & \cdots & 0 \\ 0 & 1 & -2 & \cdots & 0 \\ \vdots & \vdots & \vdots & \ddots & \vdots \\ 0 & 0 & \cdots & -2 & 1 \\ 0 & 0 & \cdots & 1 & -1 \end{bmatrix} W. \tag{24}$$

This matrix will further be denoted as D_2 (as written in the Python code).

Finally, the gradient operator with Neumann conditions ($(DW)_{i-1}$):

$$\frac{1}{h}\left[\begin{array}{cccccc} 0 & 0 & 0 & \cdots & 0 & \\ -1 & 1 & 0 & \cdots & 0 & \\ 0 & -1 & 1 & \cdots & 0 & \\ \vdots & \vdots & \vdots & \ddots & \vdots & \\ 0 & 0 & \cdots & 0 & 1 & \\ 0 & 0 & \cdots & 0 & -1 & 1 \end{array}\right] W. \tag{25}$$

3.1.7 Closed form for residuals and Jacobian

We now consider the following discrete version of the HJB equation, supplemented with the Neumann conditions and the terminal condition:

$$
\begin{cases}
-(D_t U_i)^n - \nu(\Delta_h U^n)_i + \tilde{H}(M_i^{n+1}, [\nabla_h U^n]_i) = g(x_i) + \tilde{f}_0(M_i^{n+1}), & 0 \le i < N_h, 0 \le n < N_T, \\
U_{-1}^n = U_0^n, & 0 \le n < N_T, \\
U_{N_h}^n = U_{N_h-1}^n, & 0 \le n < N_T, \\
U_i^{N_T} = \varphi(M_i^{N_T}), & 0 \le i < N_h.
\end{cases}
\tag{26}
$$

This scheme is an implicit Euler scheme since the equation is backward in time. Given M^{n+1} and U^{n+1}, we will solve for U^n. We introduce:

$$
F(U^n, U^{n+1}, M^{n+1}) = \begin{bmatrix} -(D_t U_0)^n - \nu(\Delta_h U^n)_0 + \tilde{H}(M_0^{n+1}, [\nabla_h U^n]_0) - \tilde{f}_0(M_0^{n+1}) \\ \vdots \\ -(D_t U_{N_h-1})^n - \nu(\Delta_h U^n)_{N_h-1} + \tilde{H}(M_{N_h-1}^{n+1}, [\nabla_h U^n]_{N_h-1}) - \tilde{f}_0(M_{N_h-1}^{n+1}) \end{bmatrix}
\tag{27}
$$

We solve the HJB equation using Newton-Raphson iterations:

$$
U^{n,k+1} = U^{n,k} - J^{-1}(U^{n,k}, U^{n+1}, M^{n+1}) F(U^{n,k}, U^{n+1}, M^{n+1}) \tag{28}
$$

where J is the Jacobian of $V \mapsto F(V, U^{n+1}, M^{n+1})$. We initialize $U^{n,0} = U^{n+1}$ and stop iterations when $\|F(U^{n,k}, U^{n+1}, M^{n+1})\|$ is below 10^{-12}.

The Jacobian matrix is given by:

$$
J(V, U^{n+1}, M^{n+1}) = \begin{bmatrix} \frac{\partial F_0}{\partial V_0} & \frac{\partial F_0}{\partial V_1} & \cdots & \frac{\partial F_0}{\partial V_{N_h-1}} \\ \frac{\partial F_1}{\partial V_0} & \frac{\partial F_1}{\partial V_1} & \cdots & \frac{\partial F_1}{\partial V_{N_h-1}} \\ \vdots & \vdots & \ddots & \vdots \\ \frac{\partial F_{N_h-1}}{\partial V_0} & \frac{\partial F_{N_h-1}}{\partial V_1} & \cdots & \frac{\partial F_{N_h-1}}{\partial V_{N_h-1}} \end{bmatrix}
\tag{29}
$$

Setting $C = -g(x_i) - \tilde{f}_0(M_i^{n+1})$,

Then in order to avoid numerical errors in our project we decided to take $Fi\Delta t$ and $J\Delta t$ and to avoid dividing by Δt as it will lead to numerical errors

This leads to a banded Jacobian with:

$$\frac{\partial F_i}{\partial U_{i-1}^n} = -\frac{\nu}{h^2} - \frac{1}{h^\beta}\frac{1}{(c_0 + c_1 M_i^{n+1})^\alpha}(U_i^n - U_{i-1}^n)_+ \left((U_{i+1}^n - U_i^n)_-^2 + (U_i^n - U_{i-1}^n)_+^2\right)^{\beta/2-1}, \quad (30)$$

$$\frac{\partial F_i}{\partial U_i^n} = \frac{1}{\Delta t} + \frac{2\nu}{h^2} + \frac{1}{h^\beta}\frac{1}{(c_0 + c_1 M_i^{n+1})^\alpha}\left((U_{i+1}^n - U_i^n)_- + (U_i^n - U_{i-1}^n)_+\right)\left((U_{i+1}^n - U_i^n)_-^2 + (U_i^n - U_{i-1}^n)_+^2\right)^{\beta/2-1} \quad (31)$$

$$\frac{\partial F_i}{\partial U_{i+1}^n} = -\frac{\nu}{h^2} - \frac{1}{h^\beta}\frac{1}{(c_0 + c_1 M_i^{n+1})^\alpha}(U_{i+1}^n - U_i^n)_- \left((U_{i+1}^n - U_i^n)_-^2 + (U_i^n - U_{i-1}^n)_+^2\right)^{\beta/2-1}. \quad (32)$$

Now we will extract only for the KFP equation the part that is of interest in this Jacobian : Let us denote $J_{\tilde{H}}$ the Jacobian of $U^n \mapsto \left(\tilde{H}(M_i^{n+1}, [\nabla_h U^n]_i)\right)_{0 \le i < N_h}$ evaluated in U^n.

$$(J_{\tilde{H}})_{i,i-1} = -\frac{1}{h^\beta}\frac{1}{(c_0 + c_1 M_i^{n+1})^\alpha}(U_i^n - U_{i-1}^n)_+ \left[(U_{i+1}^n - U_i^n)_-^2 + (U_i^n - U_{i-1}^n)_+^2\right]^{\frac{\beta}{2}-1} \quad (33)$$

$$(J_{\tilde{H}})_{i,i} = \frac{1}{h^\beta}\frac{1}{(c_0 + c_1 M_i^{n+1})^\alpha}\left[(U_{i+1}^n - U_i^n)_- + (U_i^n - U_{i-1}^n)_+\right]\left[(U_{i+1}^n - U_i^n)_-^2 + (U_i^n - U_{i-1}^n)_+^2\right]^{\frac{\beta}{2}-1} \quad (34)$$

$$(J_{\tilde{H}})_{i,i+1} = -\frac{1}{h^\beta}\frac{1}{(c_0 + c_1 M_i^{n+1})^\alpha}(U_{i+1}^n - U_i^n)_- \left[(U_{i+1}^n - U_i^n)_-^2 + (U_i^n - U_{i-1}^n)_+^2\right]^{\frac{\beta}{2}-1} \quad (35)$$

3.1.8 KFP Equation

To define an appropriate discretization of the KFP equation, we first discuss how to discretize

$$\partial_x \left(m(t,x)\partial_p H_0(x, \partial_x u(t,x))\right). \quad (36)$$

Recalling Neumann boundary conditions and assuming $\partial_p H(x,0) = 0$, we obtain:

$$-\int_\Omega \partial_x \left(m(t,x)\partial_p H_0(x, \partial_x u(t,x))\right) w(t,x)dx = \int_\Omega m(t,x)\partial_p H_0(x, \partial_x u(t,x))\partial_x w(t,x)dx. \quad (37)$$

A natural approximation for the right-hand side is:

$$h\sum_{i=0}^{N_h-1} M_i^{n+1}\left[\partial_{p_1}\tilde{H}(M_i^{n+1},[\nabla_h U^n]_i)\frac{W_{i+1}^n-W_i^n}{h}+\partial_{p_2}\tilde{H}(M_i^{n+1},[\nabla_h U^n]_i)\frac{W_i^n-W_{i-1}^n}{h}\right]. \tag{38}$$

Using discrete integration by parts, we get:

$$-h\sum_{i=0}^{N_h-1} T_i(U^n,M^{n+1},M^{n+1})W_i^n, \tag{39}$$

where the transport operator is as follow :

$$\begin{aligned} T_i(U,M,\tilde{M}) = {} & \frac{1}{h}\left[M_i\partial_{p_1}\tilde{H}(\tilde{M}_i,[\nabla_h U^n]_i) - M_{i-1}\partial_{p_1}\tilde{H}(\tilde{M}_{i-1},[\nabla_h U^n]_{i-1})\right] && (40)\\ & + \frac{1}{h}\left[M_{i+1}\partial_{p_2}\tilde{H}(\tilde{M}_{i+1},[\nabla_h U^n]_{i+1}) - M_i\partial_{p_2}\tilde{H}(\tilde{M}_i,[\nabla_h U^n]_i)\right]. && (41)\end{aligned}$$

We now consider the discrete version of the KFP equation (forward scheme):

$$\begin{aligned} (D_t M_i)^n - \nu(\Delta_h M^{n+1})_i - T_i(U^n,M^{n+1},\tilde{M}^{n+1}) = 0, \quad 0\le i<N_h, \quad 0\le n<N_T, && (42)\\ M_{-1}^n = M_0^n, \quad M_{N_h}^n = M_{N_h-1}^n, \quad 0<n\le N_T, && (43)\\ M_i^0 = \bar{m}_0(x_i), \quad 0\le i<N_h, && (44)\end{aligned}$$

where, for example:

$$\bar{m}_0(x_i) = \frac{1}{h}\int_{|x-x_i|\le h/2} m_0(x)dx \quad \text{or} \quad \bar{m}_0(x_i) = m_0(x_i). \tag{45}$$

3.1.9 Relationship between Transport operator and Hamiltonian Jacobian

We introduce $T(U,M,\tilde{M}) := (T_0(U,M,\tilde{M}),\ldots,T_{N_h-1}(U,M,\tilde{M}))^T$. Notice that $M\mapsto T(U^n,M,\tilde{M})$ is a linear map. Let A be the associated matrix. Then $A=(-J_{\tilde{H}})^T$.

From equation (41), we can conclude that

$$\begin{aligned} A_{i,i-1} &= -\frac{1}{h}\partial_{p_1}\tilde{H}(M_{i-1}^{n+1},[\nabla_h U^n]_{i-1})\\ A_{i,i} &= \frac{1}{h}\left(\partial_{p_1}\tilde{H}(M_i^{n+1},[\nabla_h U^n]_i) - \partial_{p_2}\tilde{H}(M_i^{n+1},[\nabla_h U^n]_i)\right)\\ A_{i,i+1} &= \frac{1}{h}\partial_{p_2}\tilde{H}(M_{i+1}^{n+1},[\nabla_h U^n]_{i+1})\end{aligned}$$

with $A_{i,j} = 0$ for $j \notin \{i-1, i, i+1\}$. Notice that

$$\tilde{H}(x, p_1, p_2) = \frac{1}{\beta} \frac{\left((p_1)_-^2 + (p_2)_+^2\right)^{\frac{\beta}{2}}}{(c_0 + c_1 x)^\alpha},$$

so that

$$\begin{aligned}
\partial_{p_1} \tilde{H}(x, p_1, p_2) &= -\frac{1}{(c_0 + c_1 x)^\alpha} (p_1)_- \left((p_1)_-^2 + (p_2)_+^2\right)^{\beta/2-1} \\
\partial_{p_2} \tilde{H}(x, p_1, p_2) &= \frac{1}{(c_0 + c_1 x)^\alpha} (p_2)_+ \left((p_1)_-^2 + (p_2)_+^2\right)^{\beta/2-1}.
\end{aligned}$$

Thus, we obtain:

$$\begin{aligned}
A_{i,i-1} &= \frac{1}{h^\beta} \frac{1}{(c_0 + c_1 x)^\alpha} (U_i^n - U_{i-1}^n)_- \left((U_i^n - U_{i-1}^n)_-^2 + (U_{i-1}^n - U_{i-2}^n)_+^2\right)^{\beta/2-1} \\
A_{i,i} &= -\frac{1}{h^\beta} \frac{1}{(c_0 + c_1 x)^\alpha} \left((U_{i+1}^n - U_i^n)_- + (U_i^n - U_{i-1}^n)_+\right) \left((U_{i+1}^n - U_i^n)_-^2 + (U_i^n - U_{i-1}^n)_+^2\right)^{\beta/2-1} \\
A_{i,i+1} &= \frac{1}{h^\beta} \frac{1}{(c_0 + c_1 x)^\alpha} (U_{i+2}^n - U_{i+1}^n)_+ \left((U_{i+2}^n - U_{i+1}^n)_-^2 + (U_{i+1}^n - U_i^n)_+^2\right)^{\beta/2-1}.
\end{aligned}$$

In other words,

$$\begin{aligned}
-A_{i,i}^T &= (J_{\tilde{H}})_{i,i}, \\
-A_{i,i-1}^T &= (J_{\tilde{H}})_{i,i-1}, \\
-A_{i,i+1}^T &= (J_{\tilde{H}})_{i,i+1}.
\end{aligned}$$

Hence, $-A^T = (J_{\tilde{H}})$.

Finally, rewriting our system:

$$M^{n+1} - M^n - \nu \Delta t D_2 M^{n+1} + \Delta t (J_{\tilde{H}})^T M^{n+1} = 0. \tag{46}$$

Thus, solving for M^{n+1} reduces to solving:

$$\left(I_{N_h} - \nu \Delta t D_2 + \Delta t (J_{\tilde{H}})^T\right) M^{n+1} = M^n. \tag{47}$$

3.1.10 Fixed Point Algorithm: A Forward - Backward system

The program consists of approximating (M, U) by fixed point iterations involving a relaxation parameter θ.

Let θ be a parameter, $0 < \theta < 1$, with typical choices being $\theta = 0.2$ or $\theta = 0.02$. Let $(M^{(k)}, U^{(k)})$ be the running approximation of (M, U). The next approximation $(M^{(k+1)}, U^{(k+1)})$ is computed as follows:

1. Solve the discrete HJB equation given $M^{(k)}$. The solution is named $\bar{U}^{(k+1)}$.
2. Solve the discrete FP equation given $\bar{U}^{(k+1)}$ and $M^{(k)}$. The solution is named $\bar{M}^{(k+1)}$.
3. Update:

$$(M^{(k+1)}, U^{(k+1)}) = (1-\theta)(M^{(k)}, U^{(k)}) + \theta(\bar{M}^{(k+1)}, \bar{U}^{(k+1)}).$$

These iterations are stopped when the norm of the increment $(M^{(k+1)}, U^{(k+1)}) - (M^{(k)}, U^{(k)})$ becomes smaller than a given threshold, say 10^{-6}.

3.2 Results

3.2.1 Parameters and consideration

We consider for the differents test the following parameters :

- $\Omega =]0, 1[$
- $T = 1$
- $g(x) = 0$
- H_0 and the discrete Hamiltonian is given by (16).
- The following sets of parameters:
  - (a) $\beta = 2$, $c_0 = 0.1$, $c_1 = 1$, $\alpha = 0.5$, $\sigma = 0.02$
  - (b) $\beta = 2$, $c_0 = 0.1$, $c_1 = 5$, $\alpha = 1$, $\sigma = 0.02$
  - (c) $\beta = 2$, $c_0 = 0.01$, $c_1 = 2$, $\alpha = 1.2$, $\sigma = 0.1$
  - (d) $\beta = 2$, $c_0 = 0.01$, $c_1 = 2$, $\alpha = 1.5$, $\sigma = 0.2$

- (e) $\beta = 2$, $c_0 = 1$, $c_1 = 3$, $\alpha = 2$, $\sigma = 0.002$

- $\tilde{f}(m(x)) = \frac{m(x)}{10}$
- $\phi(x, m) = -\exp(-40(x - 0.7)^2)$
- $m_0(x) = \sqrt{\frac{300}{\pi}} \exp(-300(x - 0.2)^2)$
- $N_h = 201$, $N_T = 100$.
- The parameter θ should be chosen such that the fixed point method converges.
- Stopping criteria in the Newton method: 10^{-12}.
- Stopping criteria in the fixed point method: 10^{-6}.

3.2.2 Graphics and general results analysis

In this section the reader may refer to Figures 2 and Figures 1

Effect of c_1 (control cost parameter): Between cases (a) and (b), we observe an increase in c_1 from 1 to 5, which means that the control cost is higher. This generally leads to a more conservative behavior in the optimal strategy. We observe that the level curves of U show a reduction in the amplitude of variations, indicating more cautious and localized decision-making. This translates into greater difficulty in terms of mass transfer for M in space. In cases (c) and (d), c_1 remains constant at 2, so the effect of the control cost is stable. This is indeed what can be observed.

Effect of c_0 (baseline control cost): Comparing (a) and (c), we note that c_0 decreases from 0.1 to 0.01. This means a reduction in the minimum cost to exercise control, encouraging more active control. This results in steeper gradients in the solutions of U, indicating faster adjustments to the dynamics of M. In (e), c_0 is set to 1, which is significantly larger, implying a more expensive control and an initial asymptotic behavior in the dynamics of M, representing this baseline control cost.

Effect of α (risk aversion parameter or weighting in the Hamiltonian function): Increasing α (as in cases (b) to (e)) means that the player becomes more sensitive to cost or risk variations. This results in more concentrated contour lines, indicating more aggressive adjustments to variations in M. This is clearly observed in the dynamics of M, with abrupt changes in the mass distribution.

Effect of σ (volatility of the underlying process): σ increases from 0.02 (cases (a), (b)) to 0.1 (case (c)), then to 0.2 (case (d)), and drops to 0.002 (case (e)). An increase in σ implies greater dispersion of agent trajectories, which tends to smooth out the solutions of M and U, reducing gradients. Conversely, for (e), σ is very low, suggesting that the solutions of U and M are more sensitive to variations in initial conditions and control effects. This is consistent with our previous observations.

3.2.3 Answer of theoretical question

Question 1 : Mass independence of state : We consider that M^n is a column vector. We recall that:

$$\left(I_{N_h} - \nu \Delta t D_2 + \Delta t (J_{\tilde{H}})^T\right) M^{n+1} = M^n.$$

Defining:

$$\gamma = I_{N_h} - \nu \Delta t D_2 + \Delta t (J_{\tilde{H}})^T,$$

and letting $v = (1, 1, \dots, 1)^T \in \mathbb{R}^{N_h}$, we aim to show that $\gamma^T v = v$. If true, this implies:

$$v^T \gamma = v^T,$$

As such we will have the following result:

$$v^T \gamma M^{n+1} = v^T M^n \Rightarrow v^T M^{n+1} = v^T M^n.$$

Expanding $\gamma^T v$:

$$\gamma^T v = \left(I_{N_h} - \nu \Delta t (D_2)^T + \Delta t J_H\right) v.$$

From equations (34)-(36), we know that the sum of coefficients of $J_{\tilde{H}}$ over any row is 0, and the same holds for D_2, leading to:

$$(\gamma^T v)_i = 1 - \nu \Delta t \cdot 0 + \Delta t \cdot 0 = 1 = v_i.$$

Thus, $\gamma^T v = v$, allowing us to conclude the proof.

Question 2: Uniqueness of solutions in discrete HJB : Let us prove the uniqueness of the solution of the discrete Hamilton-Jacobi-Bellman (HJB) equation. Suppose that $(U^n)_n$ and

$(V^n)_n$ are two solutions of the HJB equation given $(M^n)_n$. Define (n_0, i_0) such that:

$$U_{i_0}^{n_0} - V_{i_0}^{n_0} = \max_{n,i}(U_i^n - V_i^n).$$

Thus, we have the equality:

$$-(D_t U_{i_0}^{n_0}) - \nu(\Delta_h U^{n_0})_{i_0} + \tilde{H}(M_{i_0}^{n_0}, [\nabla_h U^{n_0}]_{i_0}) = -(D_t V_{i_0}^{n_0}) - \nu(\Delta_h V^{n_0})_{i_0} + \tilde{H}(M_{i_0}^{n_0}, [\nabla_h V^{n_0}]_{i_0}).$$

Rearranging:

$$\tilde{H}(M_{i_0}^{n_0}, [\nabla_h U^{n_0}]_{i_0}) - \tilde{H}(M_{i_0}^{n_0}, [\nabla_h V^{n_0}]_{i_0}) = (D_t U_{i_0}^{n_0}) + \nu(\Delta_h U^{n_0})_{i_0} - (D_t V_{i_0}^{n_0}) - \nu(\Delta_h V^{n_0})_{i_0}.$$

Since $U_{i_0}^{n_0} - V_{i_0}^{n_0}$ is the maximum possible, we obtain the inequalities:

$$\begin{aligned}(D_t U_{i_0}^{n_0}) - (D_t V_{i_0}^{n_0}) &= \frac{1}{\Delta t}\Big[- (U_{i_0}^{n_0} - V_{i_0}^{n_0}) + (U_{i_0}^{n_0+1} - V_{i_0}^{n_0+1})\Big] \le 0,\\ \nu(\Delta_h U^{n_0})_{i_0} - \nu(\Delta_h V^{n_0})_{i_0} &= \nu\frac{1}{h^2}\Big[(U_{i_0+1}^{n_0} - V_{i_0+1}^{n_0}) - 2(U_{i_0}^{n_0} - V_{i_0}^{n_0}) + (U_{i_0-1}^{n_0} - V_{i_0-1}^{n_0})\Big] \le 0.\end{aligned}$$

Thus, we obtain:

$$\tilde{H}(M_{i_0}^{n_0}, (DU^{n_0})_{i_0}, (DU^{n_0})_{i_0-1}) \le \tilde{H}(M_{i_0}^{n_0}, (DV^{n_0})_{i_0}, (DV^{n_0})_{i_0-1}).$$

Using the monotonicity of $\tilde{H}$, we finally obtain that $U^n = V^n$ for all n. Therefore, the solution to the discrete HJB equation is unique.

Question 3 : Uniqueness of solutions in discrete KFP : Let us prove the uniqueness of the solution of the discrete KFP equation. We have the equation:

$$\gamma M^{n+1} = M^n, \tag{48}$$

where $\gamma = I_{N_h} - \nu \Delta t D_x^2 + \Delta t (JH)^T$. We show that γ^T has the M-property.

- $\gamma_{i,i}^T = \gamma_{i,i} > 0$ because:

$$\gamma_{i,i} = 1 - \nu\Delta t(-1 \text{ or } -2)/h^2 + \Delta t (J_{\tilde{H}})_{i,i}^T \ge 1 + \nu\Delta t/h^2 + \Delta t (J_{\tilde{H}})_{i,i}^T > 0.$$

- For $j \neq i$, we have $\gamma^T_{i,j} \leq 0$ because:

$$\gamma^T_{i,j} = -\nu \Delta t/h^2 + \Delta t (J_{\tilde{H}})_{i,j} \leq 0.$$

- Finally, $\sum_{j=0}^{N_h-1} \gamma^T_{i,j} > 0$ because the sum of the coefficients over any row of $J_{\tilde{H}}$ and D_2 is zero.

Thus, γ^T is an M-matrix, so γ is invertible, and the solution M^{n+1} is unique.

Question 4 : Positivity propagation for M state : Let us prove that if M^0 is positive, then M^n is positive for all n. We have:

$$M^{n+1} = \gamma^{-1} M^n.$$

Since the entries of $(\gamma^T)^{-1}$ are non-negative, so are the entries of γ^{-1}. Thus, if $M^n \geq 0$, then $M^{n+1} \geq 0$. By immediate induction, $M^0 \geq 0$ implies $M^n \geq 0$ for all n.

3.2.4 A twist for $\tilde{H}$: Mean Field Control

Impact on the methodology In this section we will consider the new set of PDE, as we can observe the major change come from the $\tilde{H}(p_1, p_2, x)$ definition. As such we will apply the same methodology as before noticing that there will be another term in the residuals and the Jacobians functions for this problem :

$$\tilde{H}(p_1, p_2, \mu) = \frac{1}{\beta} \frac{\left((p_1)_-^2 + (p_2)_+^2\right)^{\frac{\beta}{2}}}{(c_0 + c_1\mu)^\alpha} - \frac{c_1\alpha}{\beta} \mu \frac{\left((p_1)_-^2 + (p_2)_+^2\right)^{\frac{\beta}{2}}}{(c_0 + c_1\mu)^{\alpha+1}}$$

Using the following set of parameters :

$$\beta = 2, \quad c_0 = 0.1, \quad c_1 = 1, \quad \alpha = 0.5, \quad \tilde{f}_0 = 0, \quad g = 0, \quad \sigma = 0.02$$

We consider factorizing by :

$$\left((p_1)_-^2 + (p_2)_+^2\right)^{\frac{\beta}{2}}$$

We can easily obtain F_i then the partial derivatives for U_i, U_{i-1}, U_{i+1} are derived as before. We conserve the transformation adopted for the transport operator and the $J_{\tilde{H}}$ is now with respect to the new coefficient.

$$F_i = -\frac{U_i^{n+1} - U_i^n}{\Delta t} - \nu \frac{U_{i+1}^n - 2U_i^n + U_{i-1}^n}{h^2}$$
$$+ \frac{1}{h^\beta \beta (c_0 + c_1 M_i^{n+1})^\alpha} \left(1 - \frac{c_1 \alpha M_i^{n+1}}{c_0 + c_1 M_i^{n+1}}\right) \left((U_{i+1}^n - U_i^n)_-^2 + (U_i^n - U_{i-1}^n)_+^2\right)^{\beta/2} + C \quad (49)$$

... and so on. $(C = 0)$

Results : In this section the reader may refer to Figures 3

Comparison between MFG and MFC:

The comparison between Mean Field Games (MFG) and Mean Field Control (MFC) reveals unexpected differences in the behavior of the solutions for U and M, especially in the structure of M under MFC. The modification of the Hamiltonian in MFC introduces a direct dependence on the mean field μ, given by:

$$\tilde{H}(p_1, p_2, \mu) = \frac{1}{\beta} \frac{\left((p_1)_-^2 + (p_2)_+^2\right)^{\frac{\beta}{2}}}{(c_0 + c_1 \mu)^\alpha} - \frac{c_1 \alpha}{\beta} \mu \frac{\left((p_1)_-^2 + (p_2)_+^2\right)^{\frac{\beta}{2}}}{(c_0 + c_1 \mu)^{\alpha+1}}$$

Unlike MFG, where agents optimize their strategies in a decentralized manner, MFC enforces a more centralized control that directly influences the distribution of the agents. However, instead of leading to smoother solutions, the resulting contours for M in MFC exhibit irregular variations and unexpected distortions. This could be due to error from our side in computation or in the code.

Figures (a) and (b) illustrate the MFG case, where the contours of U and M behave as anticipated, showing a structured and coherent evolution. However, in figures (c) and (d), representing MFC, the contours of M display erratic behavior, with abrupt variations that suggest numerical instability or unintended model effects. Which normally are smoother.

A possible explanation for this irregularity lies in the structure of the modified Hamiltonian. The term $\frac{\beta}{2}(c_0 + c_1\mu)^\alpha$ introduces a nonlinear dependency on μ, which, combined with the negative drift term $-c_1 \alpha \frac{\mu}{\beta}$, could be amplifying local fluctuations in the mass distribution. This may result in an unintended feedback loop where the control reacts too aggressively to small variations in μ, causing oscillations rather than a smooth redistribution.

Additionally, parameter choices such as α and c_1 might be playing a crucial role in destabilizing the expected mass transfer. In particular, if c_1 is too large or α is too high, the system may exhibit excessive sensitivity to local changes in μ, preventing a well-balanced control strategy.

These observations suggest that further investigation is needed to refine the MFC formulation. Adjusting the exponent α or introducing a regularization term in the control cost could help stabilize the behavior of M. Numerical improvements, such as refining the discretization scheme or using a more robust solver, might also mitigate the observed irregularities.

4 Conclusion

In this study, we have investigated a Mean Field Game (MFG) framework incorporating congestion effects, focusing on the interplay between the Hamilton-Jacobi-Bellman (HJB) equation and the Kolmogorov-Fokker-Planck (KFP) equation. Through a finite-difference discretization scheme and a fixed-point iteration approach, we have successfully implemented a numerical solution for the forward-backward PDE system.

Our results demonstrate the impact of key parameters, such as control cost, volatility, and Hamiltonian structure, on the equilibrium behavior of the system. In particular, we observed that increasing control costs leads to more conservative strategies, while higher volatility smooths out the mass distribution. The theoretical results further confirm the uniqueness and positivity preservation of the solutions under suitable assumptions.

Additionally, our extension to the Mean Field Control (MFC) setting revealed significant differences compared to MFG, particularly in the stability and structure of the population distribution. Unexpected numerical irregularities suggest that further refinements, such as improved discretization techniques or alternative regularization methods, may be necessary to obtain more robust solutions.

Overall, this work contributes to the understanding of MFGs with congestion effects and highlights the importance of careful numerical implementation in tackling forward-backward PDE systems. Future directions include exploring alternative numerical schemes, analyzing more complex interaction terms, and applying these models to real-world applications in economics and traffic flow.

5 Annexes

5.1 U contour lines

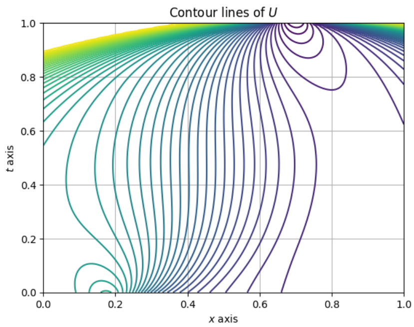

(a) $\beta = 2$, $c_0 = 0.1$, $c_1 = 1$, $\alpha = 0.5$, $\sigma = 0.02$

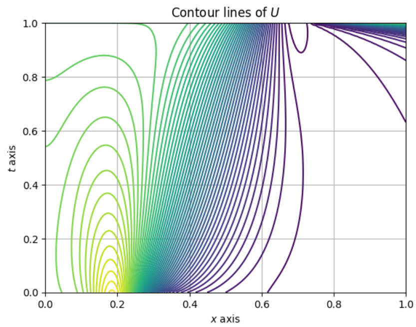

(b) $\beta = 2$, $c_0 = 0.1$, $c_1 = 5$, $\alpha = 1$, $\sigma = 0.02$

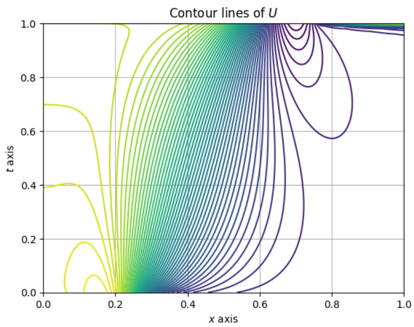

(c) $\beta = 2$, $c_0 = 0.01$, $c_1 = 2$, $\alpha = 1.2$, $\sigma = 0.1$

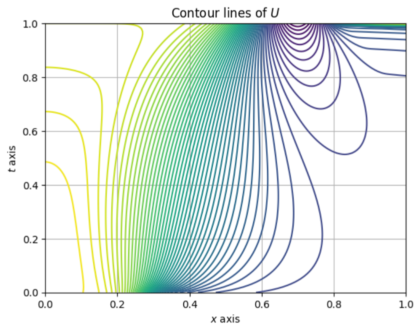

(d) $\beta = 2$, $c_0 = 0.01$, $c_1 = 2$, $\alpha = 1.5$, $\sigma = 0.2$

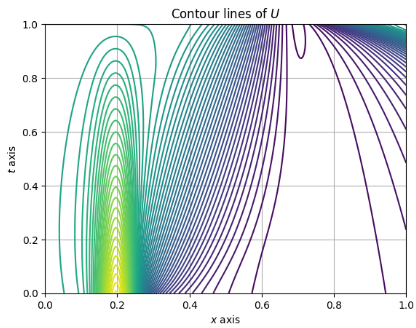

(e) $\beta = 2$, $c_0 = 1$, $c_1 = 3$, $\alpha = 2$, $\sigma = 0.002$

Figure 1: Set of graphs for contour lines for U matrix

5.2 M contour lines

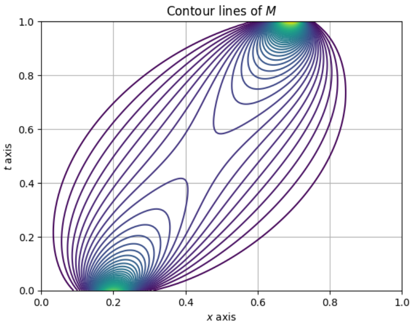

(a) $\beta = 2$, $c_0 = 0.1$, $c_1 = 1$, $\alpha = 0.5$, $\sigma = 0.02$

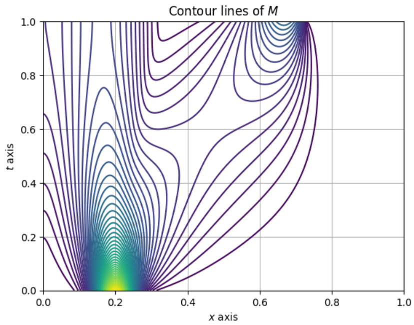

(b) $\beta = 2$, $c_0 = 0.1$, $c_1 = 5$, $\alpha = 1$, $\sigma = 0.02$

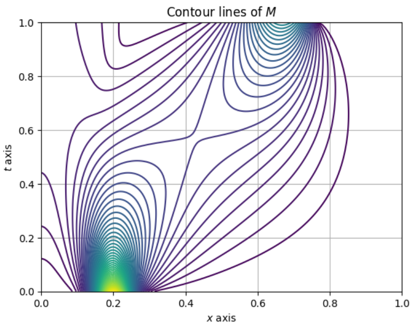

(c) $\beta = 2$, $c_0 = 0.01$, $c_1 = 2$, $\alpha = 1.2$, $\sigma = 0.1$

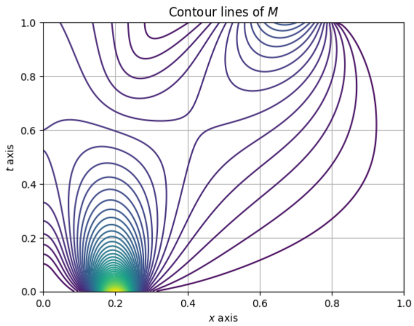

(d) $\beta = 2$, $c_0 = 0.01$, $c_1 = 2$, $\alpha = 1.5$, $\sigma = 0.2$

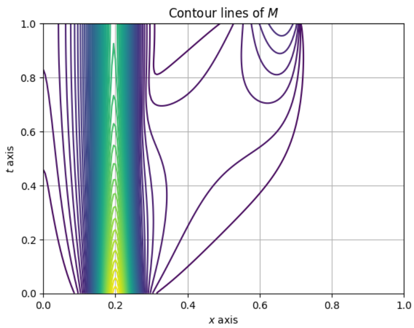

(e) $\beta = 2$, $c_0 = 1$, $c_1 = 3$, $\alpha = 2$, $\sigma = 0.002$

Figure 2: Set of graphs for contour lines for M matrix

5.3 Comparison MFG - MFC

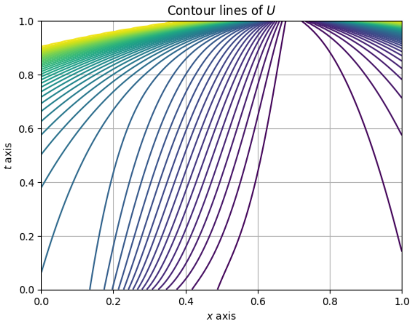

(a) MFG, U contours for : $\beta = 2$, $c_0 = 0.1$, $c_1 = 1$, $\alpha = 0.5$, $\sigma = 0.02$

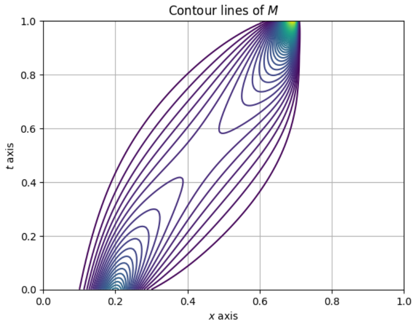

(b) MFG, M contours for : $\beta = 2$, $c_0 = 0.1$, $c_1 = 1$, $\alpha = 0.5$, $\sigma = 0.02$

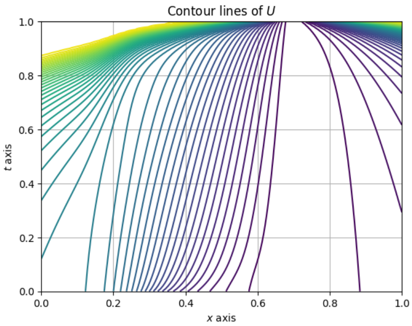

(c) MFC, U contours for : $\beta = 2$, $c_0 = 0.1$, $c_1 = 1$, $\alpha = 0.5$, $\sigma = 0.02$

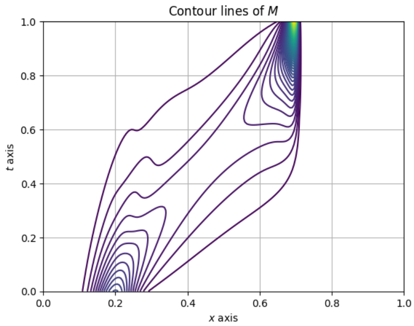

(d) MFC, M contours for : $\beta = 2$, $c_0 = 0.1$, $c_1 = 1$, $\alpha = 0.5$, $\sigma = 0.02$

Figure 3: Comparison MFG / MFC